Review

International Journal of Modern Physics A
Vol. 28, No. 30 (2013) 1330047 (25 pages)

DOI: 10.1142/S0217751X13300470

World Scientific
www.worldscientific.com

BIOLOGICAL EFFECTS ON THE SOURCE OF GEONEUTRINOS

NORMAN H. SLEEP
Department of Geophysics, Stanford University, Stanford, CA 94305, USA
norm@stanford.edu

DENNIS K. BIRD* and MINIK T. ROSING*,†
** Department of Geological and Environmental Sciences, Stanford University, Stanford, CA 94305, USA*
† Geologic Museum and Nordic Center for Earth Evolution, University of Copenhagen, Øster Voldgade 5-7, DK-1350 København K, Denmark

Received 8 October 2013
Accepted 11 October 2013
Published 28 November 2013

Detection of antineutrinos from U and Th series decay within the Earth (geoneutrinos) constrains the absolute abundance of these elements. Marine detectors will measure the ratio over the mantle beneath the site and provide spatial averaging. The measured mantle Th/U may well be significantly below its bulk earth value of $\sim$4; Pb isotope measurements on mantle-derived rocks yield low Th/U values, effectively averaged over geological time. The physics of the modern biological process is complicated, but the net effect is that much of the U in the mantle comes from subducted marine sediments and subducted upper oceanic crust. That is, U subducts preferentially relative to Th. Oxygen ultimately from photosynthesis oxidizes U(IV) to U(VI), which is soluble during weathering and sediment transport. Dissolved U(VI) reacts with FeO in the oceanic crust and organic carbon within sediments to become immobile U(IV). These deep marine rocks are preferentially subducted relative to Th(IV)-bearing continental margin rocks. Ferric iron from anoxygenic photosynthesis and oxygen in local oases likely mobilized some U during the Archean Era when there was very little O_2 in the air. Conversely, these elements behave similarly in the absence of life, where the elements occur as U(IV) and Th(IV), which do not significantly fractionate during igneous processes. Neither do they fractionate during weathering, as they are essentially insoluble in water in surface environments. Th(IV) and U(IV) remain in solid clay-sized material. Overall, geoneutrino data constrain the masses of mantle chemical and isotopic domains recognized by studies of mantle-derived rocks and show the extent of recycling into the mantle over geological time.

Keywords: Geoneutrino; subduction; uranium; plate tectonics; geochemical cycles; Pb isotopes; mantle heterogeneity.

PACS numbers: 91.45.Fj, 91.67.F−, 91.67.Fx, 91.67.Qr, 91.67.Nc, 14.60.Lm, 14.60.St

1. Introduction

Geoneutrinos are produced when beta decay of radionuclides in Earth materials emits an electron antineutrino. Here, we relate secular variations in the spatial distribution of geoneutrino fluxes from Earth to the topics of three earlier essays; *The Rise of Continents — An essay on the geologic consequences of photosynthesis*.[1] *The Hadean–Archean Environment*[2] and *Paleontology of Earth's Mantle*.[3] These essays infer that secular variations in the distribution and abundance of the radionuclides U, Th and K within Earth's mantle, crust and hydrosphere have been strongly influenced by the geochemical evolution of life's metabolic processes. Thus, one expects analogous spatial and temporal variations in the fluxes of geoneutrinos throughout the $\sim$4.5 Gy of Earth history.

Currently, detection of geoneutrinos has confirmed that radioactive decay occurs within the Earth.[4–6] Measurements are most sensitive to the decay chain of ^{238}U with a half-life of 4.468 billion years (Gy) to ^{206}Pb. Recent measurements marginally resolve the decay chain of ^{232}Th to ^{208}Pb with a half-life of 14.05 Gy.[7,8] Future improved measurements will help constrain the extent to which biological processes have facilitated geochemical separation of U from Th over geological time. Detection of neutrinos and antineutrinos from ^{40}K and antineutrinos from ^{235}U decay may eventually be feasible.[9] The rare isotope ^{235}U decays to ^{207}Pb with the half-life of 0.7038 Gy. Combined analysis of ^{207}Pb and ^{206}Pb constrains the geological age of events that affected rock samples. We consider ^{40}K, which decays to ^{40}Ar and ^{40}Ca with a half-life of 1.277 Gy, as it constrains the U and Th cycles within the Earth.

There have been dramatic secular variations in the distribution of the radioactive elements U, Th and K over geologic time leading to their preferential concentration in continental crust. Redistribution of these geoneutrino source radionuclides involves the dynamics of Earth's hydrosphere and global tectonics, including convection in the mantle. Many of the geochemical processes leading to redistribution of these elements, including the rise of continents and differential segregation of U and Th in oxic aquatic environments, have been mediated by the influence of biological processes, primarily the metabolic innovation of photosynthesis on Earth's geochemical cycles.[1–3,10–12] In this paper, we focus primarily on geochemical cycles of U and Th, and in a subsequent communication we will address biological effects on secular variations in K leading to the rise of continents. We conclude that geoneutrino measurements have the potential to determine the total extent of uranium mobility and to trace flow within the mantle.

2. Detection of Geoneutrinos

To provide context to our discussion, we briefly review the detection of geoneutrinos. Geochemical arguments constrain the average composition of the Earth's crust plus mantle "Bulk Silicate Earth" including radioactive elements U, Th and K.[13] Predictions of the geoneutrino flux at existing sites and hypothetical sites on the Earth's surface as a whole utilize these simple inferences for distant continual crust

and make simplified assumptions about the Earth's mantle.[14–18] Formally, the flux by a nondirectional detector of geoneutrinos at a site (position $\boldsymbol{r}_{\text{obs}}$) is related to the concentration of an isotope by mass as

$$F(\boldsymbol{r}_{\text{obs}}) = \int_{v_{\text{source}}} \frac{\rho(\boldsymbol{r}_{\text{source}}) C_{238}(\boldsymbol{r}_{\text{source}}) \Omega(r)}{r^2} \, dV_{\text{source}} \,, \tag{1}$$

in this case the symbol C_{238} represents ^{238}U and ρ is density, $\boldsymbol{r}_{\text{source}}$ is source position, V_{source} is source volume and Ω is a mild function of the distance from the source to observer $r \equiv |\boldsymbol{r}_{\text{source}} - \boldsymbol{r}_{\text{obs}}|$ that includes the effects of neutrino oscillations and a multiplicative constant for the efficiency of the detector at each energy level. A directional detector would involve integrals over cones with apertures depending on the resolution. A tomographic inversion would be feasible with data obtained from numerous directional detectors.

Local sources have a significant effect especially within continents where the high concentrations of radioactivity vary between rock types. There currently are far too few detectors to formally invert Eq. (1). Hence, forward modelers make testable predictions to compare with the sparse data.[14–18] They extrapolate downward from surface geological mapping and infer deep crustal structure from geophysical remote sensing to infer the production and flux of geoneutrinos.

As a consequence of chemical differentiation over Earth history, the elements K, Th and U have been strongly concentrated in the Earth's continental crust, which constitutes $\sim$0.5% of the combined mass of the crust and mantle. Presently, the continental crust contains about one-third to one-half of all the heat-producing radioactive elements and the rest are largely within the mantle.[13] Measurements of heat flux from the Earth's interior, especially in stable continental areas, help to constrain the total radioactive heat generation at crustal depths.[14,15]

3. Geologic and Biologic Perspectives of Earth History

Geological and biological processes have produced long-term geochemical trends over Earth's history that have selectively redistributed U and Th. We provide a review of the abiotic geological processes in App. A to aid the nongeological reader. Overall, the long-term abiotic trends in the evolution of Earth history are closely coupled to biological processes, with the effects of biological processes increasing over geological time.

The present Earth and its Moon formed in the aftermath of the collision between two planet-sized objects about 4.5 Ga.[19–22] Most of the mantle of Earth was initially molten and chemically well mixed. The interior mantle and the Earth's surface froze after several million years of cooling, and the oceans later condensed beneath a $\sim$100 bar atmosphere of CO_2. The chemistry of early Hadean seawater was significantly different from our present-day oceans. This Earth did not become habitable until the bulk of the CO_2 reacted with oceanic crust forming carbonate minerals and subducted into the mantle.

No intact rocks survive from these early Hadean intervals. Most of the geological information comes from studies of grains of the mineral zircon $ZrSiO_4$.[23–25] These grains formed at igneous temperatures within granitic rocks. In the Archean, these rocks were uplifted and eroded. Rivers transported the grains to where they accumulated within sandstones. Geochemists extract the zircons from metamorphosed quartzites formed from the sandstones and study their chemistry.

The distribution of elements within the Earth has changed over geological time with the formation of continental crust. The zircon studies indicate that some granitic continental masses formed by $\sim$4.4 Ga.[23,24] In addition, there is evidence of surface exposure and weathering of rock to produce clay-rich sediments[25] that later melted to form zircon-bearing granitic rocks. However, these studies do not provide useful information on the surface temperature of weathering and hence whether sterile $\sim$ 200°C conditions or clement conditions existed.

Overall processes of continental crust formation are complicated. Simply, partial melts formed within the upper mantle and ascended to shallow depths (App. A.1). These magmas were more U-rich and Th-rich than their mantle sources. Crustal processes including partial melting of hydrous rocks further concentrated U and Th into the continental crust. Erosion of continental crust produced sediments, some of which remained within continents and some of which subducted into the mantle. Subducted oceanic crust that had reacted with seawater and subducted sediments produced heterogeneities within the mantle. Biology played a key role in the fate of U and Th that we discuss in the remaining sections of this paper. Geochemists use Pb isotope from U and Th decay to track heterogeneous mantle domains over geological time (App. A.2).

An associated long-term trend is that the Earth's interior cooled over geological time (App. A.3). Within tens of million years of its formation the Earth's interior evolved into a state where heat from radioactive decay in the mantle was in crude balance with the heat that escapes from the surface (App. A.3). Decay of U, Th and K were significant from then on. The current consensus is that the Hadean mantle was a few 100 K hotter than the present mantle. Studies of the composition of mantle-derived lavas over the last three billion years give better thermal history constraints;[26–30] the mantle is cooled $\sim$150–300 K during this time span. This cooling provides a significant fraction of the heat escape from the mantle, currently 35 TW. For reference, cooling of 100 K/Gy supplies $\sim$20 TW. The remaining 15 TW comes then from radioactivity. Geochemists refer to the ratio of heat from radioactive decay in the mantle to current heat flow from the mantle as the *Urey number*; it is $15/35 = 0.43$ in the example above. It is unlikely that the mantle-cooling rate was linear. Radioactive heat production in the mantle has waned over time from the direct effect of decay and possibly from progressive transfer of these elements into the crust from the mantle.[26]

Geochemists have also used data on the elements in the Sun, in meteorites, and in terrestrial samples to deduce bulk elemental concentrations (including K, Th and U) within the Earth.[13] The present *Urey number* is less than $\frac{1}{3}$, with a compiled

range of 0.08–0.3.[16,17] Geoneutrino data are already providing a check on these inferences.[4–8] A low $\left(\ll \frac{1}{2}\right)$ value of the *Urey number*, if correct, places limits on the mean mantle heat flow and the mean rate of tectonics since the Hadean. The total heat from cooling is limited, and the observed cooling by up to 300 K used in models with plate tectonic spreading rates comparable to present ones involves most of the available mantle and core temperature change since the Earth's surface became solid very early in its history.[26–28] This inferred sluggish behavior of the Earth indicates that geochemical heterogeneities in the mantle are likely to persist for long periods of geological time.

4. Earth's Surface Uranium Cycle

We now discuss how biological surface processes have lead to geochemical conditions that have redistributed U on a global scale over geological time. We consider the process as a cycle with the obvious caveat that there has been a net redistribution and selective segregation of U and Th. There has also been a net formation of U-rich and K-rich continental crust.

Overall, the metabolic innovation of photosynthesis has utilized solar energy to reduce carbon and to oxidize the environment, ultimately leading to the rise of dioxygen in Earth's atmosphere. These effects have proven to be "Earth changing" and have significantly modified the chemistry of Earth's fluid envelopes (atmosphere and hydrosphere), crust and mantle.[1–3,11,12,31,32] For example, the majority of known minerals (including U-bearing ones) on the Earth owe their existence (directly or indirect) to reduced and oxidized regions associated with life.[11,12] We begin the uranium geochemical cycle with weathering of preexisting rocks and transport of their debris at the Earth's surface.

4.1. *Uranium solubility and mobilization*

As a consequence of photosynthesis and the rise of atmospheric dioxygen rocks on land or on the seafloor chemically weather whenever they are exposed to air or water. On land streams and rivers carry away the solid and dissolved products of weathering into the ocean. Much of this modern sediment load comes from undulant areas of the continent rather than precipitous mountains. Extensive chemical weathering occurs in flood plains during transport.[32] The dissolved species precipitate within chemical sediments such as limestones, enter clay-rich shales, or are carried into hydrothermal systems within the oceanic crust.

Since the advent of photosynthesis, uranium in minerals exposed to surfacial weathering enters the dissolved load in streams, but thorium does not. The basis for this chemical differentiation is well understood.[33] Uranium and thorium occur as U(IV) and Th(IV) in the mantle and in crustal and surface environments that have not been affected by biology. At these oxidation states the two elements behave similarly in geological processes in the Earth's interior and surface and do not significantly partition from each other. U(IV) and Th(IV) are essentially insoluble in

surface environments. They are transported mechanically within the clay fraction and within grains of trace phases such as zircon $ZrSiO_4$. Uranium has the additional available oxidation state (VI), which is modestly soluble in various forms including carbonate and SiO_2 complexes.[33] Oxidation thus separates uranium in solution from thorium in the solid. It is obvious that dioxygen suffices for this process and that there was very little dioxygen before the metabolic innovation of photosynthesis.[34]

4.2. *Geological timing of uranium mobility*

The geological timing of uranium mobility is related to the continual oxidation of ferrous to ferric iron within the Earth's crust and to the advent of dioxygen in the air. Before the advent time, photosynthesis and decay produced methane, which was a minor component in the atmosphere. Photolysis decomposed methane into H_2 and C-rich compounds that settle to the surface and were then oxidized by biology. The hydrogen ultimately came from water. The net effect of the reactions was

$$H_2O_{(\text{in ocean})} + 2FeO_{(\text{solid})} \rightarrow H_{2\,(\text{to space})} + Fe_2O_{3\,(\text{solid})}\,. \tag{2}$$

Mass balance of the Earth's crust[10] and the inferred composition of early Archean seawater[35] indicate that hydrogen in a globally equivalent layer of a few hundred meters of water was lost to space in the process. The rise of dioxygen in the air precluded significant atmospheric methane. In turn, atmospheric dioxygen could build up in part because much of the Earth's crust was already oxidized and hence not a dioxygen sink.

Geologic timing for the rise of atmospheric dioxygen is indicated by studies of the mass independent fractionation of sulfur isotopes that suggest dioxygen increased to $\sim$2 ppm at $\sim$2.45 Ga, and that the atmosphere was nearly anoxic before that time.[34,36–39] The physics is not fully understood, but the basis is not complicated. Sulfur has 4 isotopes with ^{32}S being dominant. There is a modest fraction of ^{34}S relative to ^{32}S, however fractional abundances of ^{33}S and ^{36}S are quite small. In most processes, the amount of fractionation is a function of atomic mass. Geochemists can easily measure changes in the ratio $^{34}S/^{32}S$. The ratio $^{33}S/^{32}S$ changes by $\sim 1/2$ of the amount of the $^{34}S/^{32}S$ change; the ratio $^{36}S/^{32}S$ by $\sim$2 times of the $^{34}S/^{32}S$ change. Sulfur species existed in the reduced Archean atmosphere. Ultraviolet light photolyzed these molecules, but optimal wavelength differed with each atomic mass. There were significant concentrations of ^{32}S and ^{34}S species. Light at their quantum wavelengths was absorbed high in the atmosphere, shielding the lower atmosphere; photolysis occurred primarily at high elevation. However, ^{33}S and ^{36}S were too rare to produce significant shielding so photolysis occurred over all elevations. As a consequence, the net effect separated ^{33}S and ^{36}S from the other S isotopes. This fractionation has been preserved in the Archean because the air was nearly anoxic. The fractionated material was still reduced when it was transported to

Earth's surface by atmospheric precipitation (rain) and incorporated into immobile sulfide minerals preserving the fractionation over geologic time. After the Archean, characterized by the rise of atmospheric dioxygen, sulfur oxidized to sulfate before it reached Earth's surface and dissolved in rainwater; it then entered into large well-mixed aquatic reservoirs including the ocean, offsetting any geologic record of transient fractionation.

Uranium, however, appears to have been mobile relative to thorium well before 2.45 Ga. In particular, the relative enrichment of uranium relative to thorium is observed in some of the world's oldest sedimentary rocks at Isua Greenland.[40] This organic-rich "black" shale was deposited before 3.7 Ga and strongly metamorphosed at ∼2.8 Ga. Combined analyses of the four stable Pb isotopes for a suite of samples provides the Pb isotopic composition at the time of metamorphism. The rock evolved in a high-U, low-Th environment between deposition and metamorphism. The organic matter in this shale likely reduced U(VI) dissolved in the seawater to immobile U(IV) during deposition.

Even the occurrence of the reduced mineral uraninite UO_2 appears to be influenced by biology. It occurs as a detrital mineral after ∼3.0 Ga and the oldest known in-place uraninite is 2.5–2.6 Ga.[41] Before 3.2 Ga, granitic rocks were only modestly enriched in U, Th and K and did not become saturated in uraninite during freezing from magma.[42] Calc-alkaline igneous rocks presumably from island arcs became common after this time. These rocks were more U-rich, but did not precipitate uraninite either. They did weather and were eroded. Uranium was mobilized and accumulated into organic-rich black shales by reduction to uraninite and sorption on clay minerals. These rocks then melted at crustal depths. The alumina-rich granites thus produced were sufficiently uranium-rich to crystallize uraninite.

4.3. *Archean uranium mobilization*

There are three possibilities to explain U mobility relative to Th before the 2.45 Ga date usually given for atmospheric oxidation: (1) There was significant atmospheric dioxygen in the Archean and the interpretation of sulfur isotopes is incorrect.[43] We do not discuss this possibility further as it seems in conflict with the widespread survival of reduced detrital minerals in Archean sediments.[42,44] (2) Dioxygen is not necessary to oxidize U(VI) to the mobile form of U(IV). (3) There were local dioxygen oases. The latter two hypotheses are not mutually exclusive, and attractive enough to merit discussion. Once mobilized U(VI) is likely to travel significant distances before deposition. It persists with ∼1000 yr residence-time in modern anoxic water such as in the Black Sea. In that case, absorption on clay particles is necessary for reduction to U(IV).[45]

First, life produces moderately oxidizing environments that are dioxygen free. Modern microbes have the ability to make organic matter by anoxygenic photosynthesis. Idealized reactions involve ferrous iron

$$4FeO + CO_2 + H_2O \rightarrow 2Fe_2O_3 + CH_2O \quad (3)$$

(Refs. 46 and 47) and sulfide

$$S^{2-} + 2CO_2 + 2H_2O \rightarrow SO_4^{2-} + 2CH_2O \quad (4)$$

(Ref. 48) where CH_2O is a simplified chemical formula for organic matter. Heterotrophic organisms obtain energy by reversing these reactions.[49–53] Banded iron formations in part formed from Fe-based photosynthesis, and are found within the oldest (> 3.7 Ga) known (metamorphosed) sedimentary sequences.[54] Archean black shales are likely products of anoxygenic photosynthesis. Finely disseminated sulfides are present in metamorphosed black shales from the > 3.7 Ga Isua supracrustals, possibly resulting from reduction of sulfate to sulfide by organic matter.[40] Organisms also appeared to have etched detrital pyrite FeS_2 grains at 3.4 Ga having the net effect of combined Fe-based and S-based photosynthesis.[55]

No organisms are known that use photosynthesis to make organic matter by oxidizing U(IV) to U(VI). The past and present existence of such a metabolic innovation cannot be excluded entirely based on our current state of knowledge. For example, arsenic-based photosynthesis,[56] and nitrite to nitrate photosynthesis[57] have been recently discovered. We note that there are hints of trace uranium concentrations in organic matter in living cells,[58] suggesting that further examination is warranted.

Uranium on the modern Earth is mobilized without needing dioxygen or direct anoxygenic uranium photosynthesis.[59] The process is observable when organisms first precipitate uraninite by reducing U(VI) to uraninite with organic matter. The uraninite is then oxidized by ferrous iron. The reaction written to illustrate equilibrium behavior is

$$UO_{2(\text{solid})} + 2Fe(OH)_{3(\text{solid})} + 2CO_{2(\text{gas})} + 2H^+_{(\text{aq})} \leftrightarrow UO_2(CO_3)^{-2}_{2(\text{aq})} + 2Fe^{2+}_{(\text{aq})} + 4H_2O\,. \quad (5)$$

This reaction is observed to proceed to the right in the laboratory.[59]

Thermodynamically equilibrium for any reaction depends on the presence of all the components in the reaction, but not on their modal abundance in rock or solution. We note for reaction (5) that the thermodynamic activity of the component UO_2 is less than unity if it is in solid solution within another mineral component, and that the activity of water does not deviate much from unity in most aquatic environments. Dissolution of uraninite would be favored in Archean soils where decay of organic matter produced elevated soil pCO_2 and mildly acidified water. Rain would also leach away the aqueous species on the right side of the reaction, favoring uraninite dissolution. Conversely, ferrous iron reduces U(VI) to U(IV) within the oceanic crust.[60–62] Thermodynamic calculations require attention to the actual uranium-bearing complex ions present in the water[33] as well as any solid solutions. In addition, uranium-bearing ions adsorb onto iron oxides and clays.[44,63]

Other oxidants are conceivable, for example Ginder-Vogel *et al.*[59] mention Mn oxides and nitrate as possibilities. Dismukes *et al.*[64] and Johnson *et al.*[65] suggest

that Mn-oxidizing photosynthesis predates oxygenic photosynthesis. Molecular biology indicates that the ability for life to reduce nitrate and oxidize Fe(II) predates the last common cellular ancestor, and hence photosynthesis.[66] Nitrate had to have been present for this molecular trait to evolve, and lightning is an obvious early abiotic source for modest fluxes of nitrate.

With regard to the feasibility of local oases of dioxygen, we note that dioxygen is not particularly soluble in water and has a low diffusivity. A modest dioxygen concentration in shallow water easily causes saturation at a partial pressure of $\sim$1 bar, an effect that is evident when dioxygen bubbles form on sunlit aquarium plants. Methane in modern swamps provides a relevant analog, as swamp-water and sediment pore-water quickly become saturated with respect to methane from decay of organic matter. Methane bubbles are in equilibrium with the local ambient aquatic pressure, but grossly out of equilibrium with dioxygen in the air.

In addition, the global reservoir of dissolved dioxygen in the hydrosphere is small compared with the atmosphere. The ocean ($13{,}700 \times 10^{17}$ kg) contains less than 1% of the dioxygen in the air. There is only 0.3×10^{17} kg of fresh water, mostly in a few large lakes. Assuming the oceans and fresh water have the same concentration of dioxygen suffices for an order of magnitude calculation; only 0.2 parts per million of the Earth's total dioxygen (equivalent to 0.04 ppm concentration in the air) resides in freshwater. This concentration is much less than the $\sim$2 ppm maximum limit for mass independent sulfur isotope fractionation at 2.45 Ga.[36] The equivalent atmospheric concentration residing in shallow lakes and streams is trivial. Archean streams and surface water could have been episodically oxic without significantly affecting the air. Archean flood plain waters could have been oxic during cyanobacteria blooms. Much of the modern chemical weathering of sediments occurs in flood plains during transport, rather than at outcrops.[32]

Kato *et al.*[67] suggest that the formation of hematite within 2.76 Ga basalts at $\sim$200 m depth below the paleosurface as evidence for significant dioxygen within the Archean atmosphere. Anoxygenic photosynthesis of Fe(II) could not have occurred at this depth, however, the oxidized deposit occurs within an ancient shear zone that may have provided a conduit for downward migration of oxygenated surface waters. Earthquakes transiently open through-going pore space.[68] A recent example involves sulfide oxidation at $\sim$1 km depth along the San Andreas Fault. Further support of local dioxygen oases is provided by molecular biological studies indicating that dioxygen-producing cyanobacteria evolved on land.[69–71] This inference is also ecologically attractive in that the ability to dispense with ferrous iron and sulfide of cyanobacteria is advantageous in land environments, like granitic soils, where these components have low concentrations.[72]

4.4. *Marine uranium cycle*

Streams carry weathered and eroded material from land into the ocean as both detrital grains and as dissolved solute components. Thorium and U(IV) are

transported as part of the sediment load in solid mineral grains. Coarser material accumulates preferentially in shallow near shore marine environments, while clay size particles are often transported offshore to deeper submarine basins. Rivers also transport dissolved U(VI); the global flux is estimated to be 3 to 6×10^7 mol yr^{-1}.[62] The major uncertainty is that the uranium concentration varies as a function of the lithology of the river drainage basins, for example rivers eroding regions of exposed sedimentary carbonates have higher U concentrations than those draining crystalline igneous or metamorphic rocks.[73]

Much of the uranium derived from continental masses has flowed in solution within rivers throughout geological time. We use the recent flux estimate of Morford and Emerson[74] of 4×10^7 mol yr^{-1} and data tabulated by Šrámek *et al.*[17] for illustrative purposes. There are $\sim1.32 \times 10^{17}$ mol of U within the continents, including sedimentary rocks.[17] Thus, the residence time of U is $\sim$3.3 Gy. It is reasonable that much of the continental and even mantle uranium has entered solution at some time over Earth's history.

The fate of dissolved uranium once it reaches the ocean is complicated. The mean concentration by mass (M/kg) in seawater of uranium is 3.116×10^{-9},[75] equivalent to 1.8×10^{13} mol globally. Dissolved U(VI) occurs primarily as a complex carbonate ion.[74–76] The residence time in the ocean with respect to the global river flux is thus $\sim400 \times 10^3$ yr. This time is much longer than the $\sim$1000 yr mixing time of the oceans, so one might expect that uranium would behave as a conservative component of seawater as does salinity. Normalization to a standard salinity adjusts measured U concentration for the local effects of dilution by river water and rainwater and concentration by evaporation of water from the ocean into the air. However, normalized U concentration varies as there are numerous marine transient sources and sinks.[61,74–76]

As an example, sulfide particles scavenge uranium from seawater and are deposited on the seafloor.[61] The uranium returns to solution when dioxygen in the seawater oxidizes the sulfide particles. This occurs when cool oxic seawater circulates through the shallow oceanic crust and sediments resulting in a remobilization of uranium.[61] There is a tendency for uranium to be concentrated in rocks and sediments where water moves from oxic to anoxic conditions.[42] If the oxidation front moves gradually in the reduced direction, uranium is repeatedly mobilized and deposited. Such "roll-front" type deposits are a commercial source of uranium. Subsurface microbes and organic matter are frequently but not always involved.[42]

There are two comparable long-lived significant geologic sinks for marine U(VI):[61,62,74] (1) It is reduced by organic matter that is incorporated into fine grained sedimentary rocks as U(IV) in the form of uraninite and adsorbed onto clay mineral surfaces; and (2) Seawater circulates through cool (few degrees Celsius) hydrothermal systems well away from the ridge axis, here ferrous iron in the shallow basaltic crust reduces dissolved U(VI) to U(IV). Much of this flow passes through seamounts,[77] which further augments the heterogeneity of uranium deposition in oceanic crust and the overlying sediments.

Strongly reduced sedimentary environments are not significant sinks for U today. For example, only 2% of the globally available uranium flux is sequestered within sediments beneath the Black Sea.[77] With regard to the geological past, regions of bottom anoxia expanded during Phanerozoic global marine events, and thus affected the geochemical cycle of uranium.[78,79] The fate of marine uranium has changed significantly over geological time as the oceans became more oxic.

5. Subduction of Uranium and Its Return to the Surface

We now follow the geochemical cycle of uranium from surface environments into and through the deep mantle. The oceanic crust and the overlying sediments apparently remain largely intact as they enter subduction zones. Some of this material may be scraped off and remains in the island arc, but much of it continues downward. Conversely, the subducting slab sometimes entrains crust from the overlying island arc. These chemical domains persist for geological periods of time. Below we follow their fate beginning with arc volcanism (see Fig. 2 in Ref. 2).

5.1. *Arc volcanism*

Material on top of the subducting oceanic slab becomes hotter as it descends. Hydrous minerals break down with increasing temperature, releasing water-rich fluids into the mantle material above the slab.[80–82] The top of the slab sometimes melts releasing magma directly. Studies of Pb isotopes and moderately long-lived isotopes of the U and Th decay chains constrain the fate of the material carried down by the slab. Lead, thorium and uranium are all mobile in this environment.

Some of the hydrous fluid from the slab enters the wedge between the slab and the lithosphere of the arc. This material is near the temperature of ambient mantle and too cool to melt at that depth. Introduction of water from the slab lowers its melting point. The hydrous magma formed in this manner ascends into the island arc. Th and U, preferentially enter this magma and are retained in the melt as it freezes.[80–82]

The subducting oceanic slab and the mantle wedge material above it continue downward. U- and Th-bearing hydrous fluids continue to escape upward from the slab, and the melting products from reaction of these fluids with the ambient mantle contribute to magmatism at back-arc spreading centers. Otherwise the material continues downward into the deep mantle with more fluids escaping from the slab. These fluids likely reduce the shear-wave velocity above deep slabs.[83] Mantle plumes may later encounter deep slabs and ambient mantle bearing rocks formed from these fluids.[84] The U and Th concentration of the fluids that leave the slab is difficult to model as these elements reside in trace phases including allanite in oceanic crust.[80,82]

The processes at arcs augment the heterogeneity produced by hydrothermal circulation at the ridge axis.[80–82] Subducted sediments and the uppermost oceanic crust are hydrous and CO_2-rich. From top to down, the mantle wedge is enriched in

water and CO_2 from the slab and elements carried by this fluid. The concentration of water in the wedge material adjusts to a level at which the melting point is not significantly depressed. That is, the final water concentration is between that of a major and minor element. Incompatible trace elements may be enriched by factors of $\sim$100 over bulk mantle. These regions preferentially melt whenever flow in the mantle returns them to shallow depths.

5.2. *Return of subducted material through the mantle to the surface*

Subducted material continues downward with the slab. Geometrically it is inevitable that much of this material eventually returns to shallow environments. Mass balance relationships constrain the cycle time for mantle material. For example, current plate production rate is $\sim$3 km^2 of surface area per year, and in round numbers, the slab is $\sim$100 km thick and it entrains material on both its sides with an effective total thickness of $\sim$200 km. Upper mantle density is $\sim$3300 kg m^3, and the mass rate is 2×10^{15} kg yr^{-1}. The mass of the mantle is 4×10^{24} kg, so the slab cycle time is $\sim$ 2 Gy, compared with the $\sim$4.5 Gy age of the Earth since the moon-forming impact.

The mantle is chemical and isotopically heterogeneous on all scales, but sampling problems clearly exist in terms of trying to characterize the heterogeneities.[85–90] Petrologists can study mantle-derived magmas, mostly those that erupt as lavas, mantle rocks (xenoliths) that are entrained by magmas, and mantle that has been tectonically exposed.

Low-volume magmas preferentially sample easily melted domains. Such melting occurs beneath the lithosphere in mid-plate regions. Diamond pipes (kimberlites, in the broad sense) forming at $\sim$200 km depth are the deepest available magmas. These fluids are very CO_2- and H_2O-rich. Diamonds, mineral inclusions within diamonds, rock xenoliths and the magma itself sample small mantle heterogeneities. The Th/U ratio ($\boldsymbol{\kappa}$) of the kimberlite source regions of the mantle calculated from the composition of kimberlite zircons has decreased from the bulk silicate Earth value of $\sim$4 at 2.55 Ga to $\sim$2 at present, as expected from the preferential subduction of U relative to Th as the Earth's surface became more oxic.[90] The $^{13}C/^{12}C$ ratio within diamonds is heterogeneous; some samples have the bulk mantle value while many have the range expected from subduction of organic matter and carbonates.[3,84,91–93]

Still biological effects are evident within basalts associated with significantly voluminous partial melting. The measured value of the ratio $\boldsymbol{\kappa}$ = Th/U is $\sim$2.5 while the value of $\boldsymbol{\kappa}$ computed from the initial meteorite lead isotopic ratios and the measured isotopic ratios defines the Bulk Silicate Earth value of $\boldsymbol{\kappa} = 4$. This "kappa conundrum" is only a problem if one regards the mantle as a closed system.[85–90] It is readily explained if U has been preferentially subducted into the mantle as the Earth's surface environments became oxic due to biological processes.

There are broad isotopic provinces for mantle derived-magma. The DUPAL province includes much of the South Atlantic and Indian oceans.[87,88] There are

locally similar rocks at the spreading ridge in the Arctic Ocean.[94] The source in this case is possibly continental lithospheric mantle that foundered into the convecting mantle during continental break-up. Stagnated old slabs are another possible source.[84] In addition, hydrous fluids that escape from deep slabs have been detected by tomography.[83] An attractive hypothesis is that these fluids react with the ambient upper mantle and are eventually carried into the melting region beneath mid-oceanic ridge axes.[95,96] The enriched mid-oceanic ridge basalts (EMORB) are thus enriched in those incompatible elements that tend to enter slab fluids relative to normal mid-ocean ridge basalts (NMORB). Both NMORB and EMORB form by large fractions of partial melting beneath ridge axes. Studies of Pb and other radiogenic isotopes indicate that the residence time for the EMORB source is $\sim$300 My.[96]

5.3. *Provenance of mantle source regions*

The objective is to use geochemistry to trace mantle magma source regions to a particular subduction zone. At present, petrologists can trace the environment and age of the subduction zone, but not its location. Here, we discuss two examples easily related to biology to illustrate the reality of the return of subducted surface material. We then discuss a more complicated one.

The HIMU (high μ, $^{238}U/^{204}Pb$) mantle end-member is well sampled within lavas on oceanic islands including those of the southwestern Pacific Ocean and St. Helena in the Atlantic. $^{206}Pb/^{204}Pb$ is as high as 22.[94] Sulfur in these lavas shows mass independent sulfur isotopic fractionation.[97] That is, the subducted source of the lavas was likely before the rise of atmospheric dioxygen $\sim$2.45 Ga and it included altered oceanic crust as well as its overlying sediments. The subducted material lost Pb to hydrous fluids at the island arc and is hence lead poor rather than exceptionally uranium rich. Subducted material then entered the lower mantle before ascending in a mantle plume and erupting $\sim$20 Ma.

Thallium has two stable isotopes with no significant radiogenic component within Earth, ^{203}Tl and ^{205}Tl. These isotopes fractionate when cold oxic (few degree C) fluids circulate through the oceanic crust. ^{205}Tl is preferentially incorporated in submarine manganese nodules. The ratio $^{205}Tl/^{203}Tl$ is thus high within the manganese nodules and low within the uppermost oceanic crust.[98] Nielsen *et al.*[99] recently found fractionated thallium isotopes along with subducted chemical signatures of manganese nodules and altered uppermost oceanic crust as domains within Hawaiian lavas. Subducted material was on the seafloor after 1.85 Ga when the deep ocean became somewhat oxic.[100–103] The slab entered the lower mantle, and the material recently ascended within the Hawaiian mantle plume.

Hypersaline seas form when continental break up occurs within an arid region, and nascent ocean basin was initially poorly connected to the open oceans. Evaporation saturates the water with halite, NaCl. Oceanic crust reacts with this hydrothermal fluid. Eventually the new ocean becomes wide enough that seawater has good access ending deep-water halite deposition. The modern Red Sea passed

through these stages in the last few million years. Hypersaline margins eventually enter subduction zones, in that the last part of the slab before the trench collides with the continental margin includes this NaCl-rich material. This sequence of events is potentially observable in the continental geological record. Mineral inclusions in diamonds from the Juina area of Brazil are attractive indications of subducted hypersaline material. Minerals include halite (NaCl) as well as sodium-carbonates and sulfates.[103,104] Negative $\delta^{13}C$ in the Juina diamonds is compatible with subduction of organic matter.[84,103,104] For context, the eruption ages of all of these Juina kimberlites are in the range of 92–95 million years, and the subduction age of the source region is unknown. These diamonds also contain high-pressure minerals, indicating that the source region traversed the lower mantle possibly within a mantle plume.[84,103–106]

Other sources have been suggested for the Juina diamonds. Harte and Richardson[84] inferred that a mantle plume entrained material from a Mesozoic subducted slab beneath Brazil that had not yet sunk to the base of the mantle. However, crust from the open Pacific Ocean has subducted beneath Brazil, so there is no evident locality for subducted hypersaline seafloor. One could contend that mantle processes mimicked the chemistry expected from hypersaline crust. Palot *et al.*[107] invoked primordial mantle heterogeneities. This possibility cannot be excluded given the collective ignorance of the nascent Earth.

Overall, geoneutrino data provide spatial averages that supplement the time averages provided by Pb isotopes on tiny samples. At a minimum, a marine geoneutrino detector will provide an instantaneous value of κ in the mantle beneath the site. A value much less than the BSE value of $\sim$4 indicates that much of the mantle U has passed through surface environments; that biological processes fractionated U from Th, and that seafloor rocks bearing mobilized U subducted into the mantle. Conversely, variations in geoneutrino κ for continental crust indicate in turn that the parent materials for these rocks passed through surface biological environments.

6. Potassium and Nitrogen Cycles

^{40}K atoms produce geoneutrinos that currently cannot be detected. We provide a brief discussion as detection of potassium geoneutrinos may eventually be feasible and as coupling of potassium with nitrogen bears on provenance. The potassium surface and mantle cycles are coupled with the nitrogen cycle and hence to biological processes.

Abiotically, K is an incompatible element that is concentrated within magmas and hydrous fluids escaping from oceanic crust and overlying sediments during subduction. Like U and Th, much of the Earth's K has accumulated in the continental crust and its sediments over geological time. Potassium is an important component of common clay minerals that form during weathering of continents, runoff leads to deposition within marine shale. Shale is later metamorphosed into crystalline metamorphic rocks and melted to form granites. As already noted, re-melting of organic U-rich sediments leads to uraninite-bearing granites.[42]

Ammonium (NH_4^+) commonly substitutes for K^+ in silicate minerals. This process occurs within clays in agricultural soils[108] and low-temperature hydrothermal deposits.[109] Ammonium within silicate minerals is stable at metamorphic[110,111] and igneous conditions.[112] The presence of ammonium within metamorphosed sediments of $>$ 3.7-Ga-old Isua locality in Greenland indicates its durability.[111] Ammonium-bearing silicates are stable at very high pressures, indicating that subducted NH_4^+ can traverse the mantle.[113,114]

Mantle-derived nitrogen provides both an indication of potassium subduction and the timing of this subduction. The abiotic physics is straightforward. Ammonia within solid silicates breaks down at high-temperatures by contact with basaltic magmas

$$2NH_{3\,(\text{in silicate})} \leftrightarrow N_{2\,(\text{in fluid or magma})} + 3H_{2\,(\text{in fluid or magma})}\,. \tag{6}$$

The presence of K-minerals stabilizes ammonia by crystallographic substitutions forming a solid solution. Break down of these minerals releases N_2, K and H_2 that are dissolved in magmas aqueous-rich fluids. N_2 then behaves like a rare gas. ^{40}Ar produced from ^{40}K decay also escapes into the magma or aqueous fluids. The concentration of N_2 in lavas correlates with ^{40}Ar as expected from this hypothesis[115,116] (Fig. 1). It does not correlate with the primordial rare gases ^{36}Ar and ^{38}Ar. Thus extant mantle nitrogen is not a primordial component of the mantle.

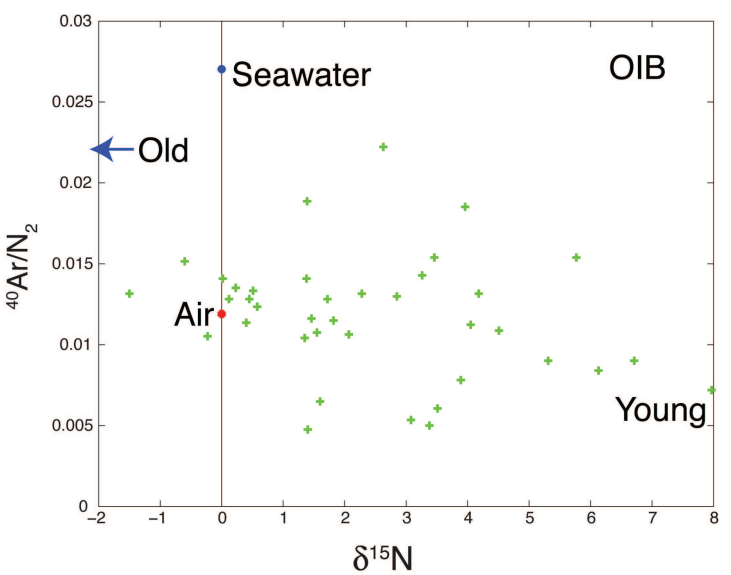

Fig. 1. The $^{40}Ar/N_2$ for samples from oceanic islands including Iceland–Hawaii-seamounts. Samples derived from recently subducted material should have low $^{40}Ar/N_2$ and high $\partial^{15}N$. Samples derived from Archean subducted material should have high $^{40}Ar/N_2$ and low $\partial^{15}N$. Mixing trends are essentially straight lines. The ocean is a minor nitrogen and argon reservoir compared with the air and the mantle (data from Ref. 115). OIB, ocean island basalt.

Most of the subducted ammonium is biologically generated within organic-rich sediments. The rare isotope ^{15}N fractionates from the common isotope ^{14}N, and geochemists express this variation as $\delta^{15}N$ in parts per mil relative to the atmospheric standard. $\delta^{15}N$ in sediments was negative in the Archean, when the atmosphere and ocean were anoxic, and positive thereafter, when conditions were oxic.[115,116]

Conversely the correlation of potassium with nitrogen indicates that a significant portion of potassium in the mantle was subducted within sediments and the altered uppermost oceanic crust. The half-life of ^{40}K is $\sim$1.248 Ga. Material subducted in the Archean should have high $^{40}Ar/N_2$ and negative $\delta^{15}N$; more recent material should have low $^{40}Ar/N_2$ and positive $\delta^{15}N$. There is some tendency for this to be so (Fig. 1), but most of the $\delta^{15}N$ values are positive, indicative of a post-Archean source. That is, negative $\delta^{15}N$ values as observed in diamonds[115,116] indicate the persistence of Archean subducted material in the mantle, but that this material is not abundant enough to strongly affect the bulk $\delta^{15}N$ of the lavas plotted in Fig. 1. Conversely, significant mantle K has never passed through the crust.[117] The ^{40}Ar associated with this potassium would have likely escaped to and remained in the atmosphere. Potassium cycling and crustal composition models that produce excessive atmospheric ^{40}Ar can be rejected.

7. Concluding Remarks

Earth's mantle is highly heterogeneous. We prefer the testable least-astonishing hypothesis that many of these heterogeneities are a consequence of subduction of sediments and altered uppermost oceanic crust. Uranium became increasingly mobile relative to thorium as surface environments became more oxic over geologic time due to the metabolic innovation of photosynthesis. Parts of the mantle and crustal rocks formed at the expense of black organic-rich shales should thus have Th/U significantly less than the Bulk Silicate Earth value of $\sim$4. Conversely, high Th/U crustal rocks formed as uranium was leached out. Such reservoirs certainly exist, but sampling is limited to rocks that have come near Earth's surface.

The geochemical behavior of uranium, and even thorium, are not ideal for modeling. There is evidence for U(VI) to enter into solution in the oldest preserved marine sediments at $\sim$3.8 Ga,[40] well before the rise of dioxygen in the atmosphere ($\sim$2.4 Ga), suggesting that there were local oases of oxic environments. Both U and Th enter trace phases or are sorbed onto the surfaces of minerals, making thermodynamic calculations difficult. Uranium is repeatedly mobilized and deposited in oxic environments with anoxic domains. Fluids carry unknown amounts of U and Th out of the slab during subduction. Lead isotopic studies provide information of trace element ratios but not absolute concentrations. Diamonds and low-volume lavas sample tiny fractions of the bulk mantle. It is therefore not straightforward to determine even the composition of present-day crust and mantle, or secular variations in the distribution of U and Th over geologic history.

Statistical analysis of rock samples is analogous to appraising a gold-bearing gravel deposit. For simplicity, the grains are 1 g; 10^{-6} of the grains are gold nuggets. In a 1-tonne sample of the gravel, 1 nugget is expected on average. However, there may be none or several. One does not *a priori* know the statistical distribution of Au in the gravel. It may be skewed with numerous nuggets concentrated in pockets. From the central limit theorem, little can be learned about the tails of distributions from their centroids.[118] Here, the tails of U and Th distribution in the Earth may contribute a minor or a major fraction of the total. Huang *et al.*[18] address the problem of distribution tails in the crust.

Geoneutrino data are very useful for studying the Earth in that they are weighted averages centered on the detectors (Eq. (1)). The current best results constrain U mainly in the crust below Japan[8] and Italy.[7] These results are compatible with geological predictions.[5–9,14–18] There are no large "hidden" uranium reservoirs in the crust and nearby mantle at these localities. The mantle contribution to geoneutrino flux is small, as expected if the Urey ratio of current mantle radioactivity to mantle heat flow is much less than $\frac{1}{2}$. This confirms petrological inferences that the interior of the Earth has cooled over geological time. The best current measurements[7,8] marginally resolve a contribution from Th geoneutrinos and hence do not provide evidence on biological fractionation of these elements. It is likely that future detectors and longer counting times will produce useful information with Th and perhaps eventually K.

Acknowledgments

We thank the participants of the 2013 Neutrino Geoscience Conference in Takayama, Japan, for feedback. The Stanford University School of Earth Sciences provides Allan Cox Visiting Professorship for M. T. Rosing.

Appendix A. Global Physical Process

We review in this appendix the largely abiotic processes that have redistributed U and Th within the Earth over geological time. We then discuss lead isotopic methods and heat flow studies that provide information on these processes including the formation of the Earth's crust to place the discussion of biological processes in context.

A.1. *Physics of mantle melting*

We begin with a brief discussion of the physics of melting, concentrating on U and Th.[119–123] The upper mantle is not a eutectic mixture; the fraction of melting increases with temperature at a given pressure between its solidus and liquidus. The melting point gradient in the upper mantle is steeper than the adiabatic gradient. Water and CO_2-rich domains melt first with increasing temperature upon heating and with decreasing pressure on ascent. Trace components with high

oxidation states and large ionic radii, including ThO_2 and UO_2, preferentially enter basaltic magmas. Geochemists refer to the class of elements that preferentially enter melts as "incompatible." High fractions of melting occur beneath mid-oceanic ridge axes where ambient mantle ascends adiabatically to the base of the oceanic crust at ∼6 km depth and also within mantle plumes that ascend from very deep in the mantle. Plume material is ∼300 K hotter than ambient mantle. We begin our discussion below with deep-source low-volume regions and work upward.

Basaltic magma erupts in mid-plate regions including Hawaii, and at mid-oceanic ridge axes. Low-volume melts erupted above moderately thick lithosphere sample modest-sized mantle heterogeneities. Voluminous melts formed at ridge axes pond within magma chambers. Their mantle source region is above the depth (currently ∼56 km, ∼50 km below 6 km thick crust[120]) where the adiabatic gradient for mantle material intersects the melting curve of anhydrous mantle.

Plates diverge at ridge axes and hot mantle material upwells to replace the material that spreads laterally to form oceanic lithosphere. Off-axis the lithosphere slowly cools from top to down by conduction. Except at very slowly spreading ridges ($\lesssim$20 mm a^{-1} full rate), mantle ascends rapidly enough at ridge axes that it loses little heat by thermal conduction, however, a column of adiabatic ascending material is a good approximation. The oceanic crust forms at the top of the column when the basaltic magma freezes. Thermal conduction inefficiently cools the deep crust at fast ($\gtrsim$60 mm a^{-1} full rate) spreading ridge axes. A steady state magma chamber consisting of a thin (tens of meter) magma lens over a (few kilometer thick) chamber of mostly crystalline mush exists at the axes. Ascending magmas pool within the lens. Hydrothermal circulation through the solid crust above the lens removes heat. The magma within the lens partly crystallizes as it cools; the crystals fall to the floor of the lens. The mush in the chamber flows downward and laterally with as the seafloor spreads away from the magma chamber. It freezes to solid gabbro a few kilometers from the axis.

A thin 0.5 to 2 km lid region above the lens is formed by magmas that ascended from the lens and froze quickly. The bottom part of this layer is dikes that intruded and the upper part is preferentially frozen lava flows. These basalts are enriched in incompatible elements including U, and Th that did not enter the gabbro forming at the base of the lens. That is, incompatible elements including U and Th concentrate in the upper 0.5–2.0 km from an initially ∼56 km column. They are enriched abiotically relative to the initial mantle by a factor of 28–100.

Overall the process has the net affect of pooling melt in magma chambers, hence destroying previous mantle heterogeneities. It abiotically creates new heterogeneities. Partial melting strongly depletes the residuum beneath the crust from melting in K, Th and U, as well as H_2O and CO_2. This partition has little immediate effect on geoneutrino flux as a column of unmelted mantle beneath the residuum as the same overall composition as the column of residuum plus the oceanic crust.

A.2. *Lead isotope systematics and the fate of U and Th*

For all elements that have a significant radiogenic component, their isotopic ratios are highly heterogeneous within the Earth on all scales. Domains within even the convecting mantle of the Earth remain chemically distinct for geological periods of time.[85–88] Geochemists have studied radiogenic Pb since soon after the discovery of radioactivity, and the chemistry of the Pb isotopic system is well constrained. For our purposes, Pb isotopic systematics provide constraints on the long-term U and Th composition of crust and mantle reservoirs, as well as absolute ages. These data augment the instantaneous measurement of geoneutrinos.

Geochemists measure the daughter isotopes ^{206}Pb, ^{207}Pb and ^{208}Pb and parent isotopes ^{232}Th, ^{235}U and ^{238}U. The isotope ^{204}Pb is essentially stable and has no significant radioactive parent, and geochemists use it to normalize concentrations of the other isotopes, for example, $\mu \equiv {}^{238}\mathrm{U}/{}^{204}\mathrm{Pb}$.

Meteorites provide a simple example of how Pb isotope variations evolve. These rocks formed over a brief period early in the history of the solar system. Sulfide grains are very rich in Pb and have very little U and Th. They essentially retain their starting of ^{206}Pb/^{204}Pb, ^{207}Pb/^{204}Pb and ^{208}Pb/^{204}Pb. There are slight variations,[15] which we ignore for brevity. The ratios ^{206}Pb/^{204}Pb, ^{207}Pb/^{204}Pb and ^{208}Pb/^{204}Pb increased over time within other Pb-poor, Th-rich and U-rich meteorite grains that behaved as closed systems. For example, points on a diagram plotting ^{206}Pb/^{204}Pb as a function of ^{238}U/^{204}Pb will define a straight line called an isochron, with the lower end at the starting Pb isotopic ratios. The slope of the isochron yields the age. However, recent mechanical mixing of two unrelated samples also produces a line on an isochron plot that does not provide straightforward information on the age. Self-consistency checks are available. Three isochron ages arise from the daughter-parent pairs: ^{206}Pb/^{204}Pb–^{238}U/^{204}Pb, ^{207}Pb/^{204}Pb–^{235}U/^{204}Pb and ^{208}Pb/^{204}Pb–^{232}Th/^{204}Pb. Ages from other isotopic systems and relative geological ages provide further self-consistency.

Existence of two uranium isotopes allows obtaining an age that is not affected by recent loss of Pb from the sample during weathering that affects the concentration of Pb relative to Th and U, but not Pb isotopic ratios. The half-life of ^{235}U (0.7038 Gy) is much less than that of ^{238}U (4.468 Gy). As a consequence, the ratio ^{207}Pb/^{204}Pb (relative to ^{206}Pb/^{204}Pb) increased rapidly early in the Earth's history when there still much ^{235}U around, but increases slowly now for a given value of μ. A suite of points on a ^{207}Pb/^{204}Pb versus ^{206}Pb/^{204}Pb plot defines an isochron for an otherwise closed system that has recently lost Pb.

This Pb–Pb dating method provides reliable ages only if ratio ^{238}U/^{235}U differs very little between samples. This ratio does vary slightly among meteorites and needs to be measured for precise ages.[124,125] In addition, this ratio also varies slightly among terrestrial samples except for rare cases where natural nuclear reactors have formed in the geological past.[126,127] The deviations of at most parts per thousand of ^{238}U/^{235}U from its typical value of 137.818 can be associated with

fractionation mainly during redox reactions.[126,127] Resolution of the expected fractions of parts per thousand variation of $^{238}U/^{235}U$ due to biological process is impractical. The detector would have to count millions (1000^2) of ^{235}U geoneutrinos, which are currently undetectable.

Near constancy of the $^{238}U/^{235}U$ ratio is evidence against the hypothesis that large natural reactors are significant heat sources within the Earth's interior.[128] One could, however, propose a "hidden reservoir" that does not supply material to the parts of Earth that can be sampled. Geoneutrino data directly limit the size of any putative hidden reservoirs. Here, the energy spectrum of natural reactor antineutrinos differs from that of uranium and thorium series geoneutrinos.

The pair $^{208}Pb/^{204}Pb$–$^{206}Pb/^{204}Pb$ behaves similarly to $^{207}Pb/^{204}Pb$–$^{206}Pb/^{204}Pb$ if the present atomic ratio $\kappa \equiv {}^{232}Th/^{238}U$ does not vary much. Such behavior is expected if the only available oxidation states are Th(IV) and U(IV), as is likely in the absence of biological activity. A main thesis of this paper is that U(VI) forms within oxidized environments that have been affected by life, specifically the metabolic waste products of photosynthesis and subsequent rise of oxygen in Earth's atmosphere. U(VI) is soluble in clement water, and streams transport it toward the ocean where it is eventually reduced to the insoluble form of U(IV) which accumulates in organic-rich sediments and the uppermost oceanic crust. Plate movements eventually result in U subduction into the mantle (see discussion below). Pb isotope measurements of samples from the crust and from mantle-derived rocks confirm that mobilization of uranium relative to thorium has occurred.[85–89] The range of Pb isotope ratios is large, easily measured and not significantly affected by isotopic fractionation. For example, Stracke (Fig. 1, Ref. 94) reports $^{206}Pb/^{204}Pb$ from 17 to 22, $^{207}Pb/^{204}Pb$ from 15.3 to 15.85 and $^{208}Pb/^{204}Pb$ from 37 to 41.5 for a global suite of mantle derived lavas. Geoneutrino measurements thus have the potential to determine the total extent of uranium mobility and to trace flow within the mantle.

A.3. *Mantle heat budget and radioactivity*

Radioactive heating of the Earth's interior provides additional long-term constraints related to the production and flux of geoneutrinos. Half-lives of heat producing isotopes ^{232}Th, ^{238}U, ^{40}K and ^{235}U are crudely comparable to the $\sim$4.5 billion years of Earth history before present (Ga). Thus, global production of radioactive heat has waned gradually through time. There is thus an urge to suppose that the global rate of seafloor spreading (and tectonics in general) was much higher on early Earth than at present. In general, this should be avoided, except for very early times following the moon-forming impact at $\sim$4.5 Ga, which left much of the Earth molten and very rapidly convecting. Rather, cooling of the Earth's interior over time has been a significant heat source.

Geodynamicists model the global heat budget of the mantle separately from radioactive heating due to the concentrations of U, Th and K in continental crust.

Heat from that latter source quickly (tens of million years) escapes to the surface and is measured in terrestrially heat flow studies.[14,15] Heat flow associated with cooling of the oceanic lithosphere is the dominant loss from the mantle. The average heat flow depends inversely on the square root of the age of the lithosphere at subduction, and is currently $\sim$0.1 W m^{-2} on average over the 60% of the Earth covered by ocean basins, with a current average lifetime is $\sim$100 My (million years). About 0.02 W m^{-2} on average escapes from the mantle beneath continents. So the average heat flow from the mantle is $(0.10 * 0.6 + 0.02 * 0.4) = \sim 0.068$ W m^{-2}. The area of the Earth is 5.1×10^{14} m^2 so the total mantle heat flux is $\sim$35 TW. This heat flux $Q_{\rm surf}$ is supplied by radioactivity and cooling of the Earth, expressed as:

$$Q_{\rm surf} = \int_{\rm Earth} \sum_{\rm rad} C_{\rm rad} H_{\rm rad} \rho \, dV - \int_{\rm Earth} \rho C \frac{\partial \Gamma}{\partial t} dV \equiv Q_{\rm rad} + Q_{\rm cool} \,, \quad \text{(A.1)}$$

where $C_{\rm rad}$ is the concentration of a radioactive element, $H_{\rm rad}$ the heat production per mass of that element, ρ is density, C is heat capacity, T is temperature and t is time.[26] The volume integrals are taken over the Earth except for the continental crust. They also may be taken over the mantle as a whole; if so, heat flux from the core to the mantle and the cooling of the core must be included in the model. The Urey ratio, defined as $U \equiv Q_{\rm rad}/Q_{\rm surf}$, is widely used in geodynamics and geochemistry as a measure of the current importance of radioactive heating. Present surface heat flow as expressed by Eq. (A.1) is well constrained. A major task of geodynamics is to estimate the rate of past plate movements and hence past heat flow. Direct estimates from the lifetimes of geological features are comparable to the present ones.[26,129]

References

1. M. T. Rosing, D. K. Bird, N. H. Sleep, W. Glassley and F. Albarede, *Palaeogeogr. Palaeoclimatol. Palaeoecol.* **232**, 99 (2006).
2. N. H. Sleep, *Cold Spring Harb. Perspect. Biol.* **2**, a002527 (2010).
3. N. H. Sleep, D. K. Bird and E. Pope, *Annu. Rev. Earth Planet. Sci.* **40**, 277 (2012).
4. T. Araki *et al.*, *Nature* **436**, 499 (2005).
5. A. Gando *et al.*, *Nature Geosci.* **4**, 647 (2011).
6. N. Tolich, *Nucl. Phys. B* (*Proc. Suppl.*) **229–232**, 407 (2012).
7. G. Bellini *et al.*, *Phys. Lett. B* **722**, 295 (2013).
8. A. Gando *et al.*, *Phys. Rev. D* **88**, 033001 (2013).
9. S. T. Dye, *Rev. Geophys.* **50**, RG3007 (2012), doi:10.1029/2012RG000400.
10. C. Lecuyer and Y. Ricard, *Earth Planet. Sci. Lett.* **165**, 197 (1999).
11. R. M. Hazen *et al.*, *Am. Mineral.* **93**, 1693 (2008).
12. D. Papineau, *Elements* **6**, 25 (2010).
13. W. F. McDonough and S. Sun, *Chem. Geol.* **120**, 223 (1995), doi:10.1016/0009-2541(94)00140-4.
14. H. K. C. Perry, J.-C. Mareschal and C. Jaupart, *Earth Planet. Sci. Lett.* **288**, 301 (2009).
15. J. C. Mareschal, C. Jaupal, C. Phaneuf and C. Perry, *J. Geodyn.* **54**, 43 (2012).
16. O. Šrámek, W. F. McDonough and J. G. Learned, *Adv. High Energy Phys.* **34**, 235686 (2012), doi:10.1155/2012/235686.

17. O. Šrámek, W. F. McDonough, E. S. Kite, V. Lekić, S. T. Dye and S. Zhong, *Earth Planet. Sci. Lett.* **361**, 356 (2013), doi:10.1016/j.epsl.2012.11.001.
18. Y. Huang, V. Chubakov, F. Mantovani, R. L. Rudnick and W. F. McDonough, *Geochem. Geophys. Geosyst.* **14**, 2003 (2013).
19. R. M. Canup, *Icarus* **168**, 433 (2004).
20. R. M. Canup, *Science* **338**, 1052 (2012).
21. M. Ćuk and S. T. Stewart, *Science* **338**, 1047 (2012).
22. K. Zahnle, N. Arndt, C. Cockell, A. Halliday, E. Nisbet, F. Selsis and N. H. Sleep, *Planet Space Sci. Rev.* **129**, 35 (2007).
23. M. D. Hopkins, T. M. Harrison and C. E. Manning, *Earth Planet. Sci. Lett.* **298**, 367 (2010).
24. T. M. Harrison, *Annu. Rev. Earth Planet. Sci.* **37**, 479 (2009).
25. A. J. Cavosie, S. A. Wilde, D. Liu, P. W. Weiblen and J. W. Valley, *Precambrian Res.* **135**, 251 (2004).
26. J. Korenaga, *Rev. Geophys.* **46**, RG2007 (2008), doi:10.1029/2007RG000241.
27. C. Herzberg, P. D. Asimow, N. Arndt, Y. Niu, C. M. Lesher, J. G. Fitton, M. J. Cheadle and A. D. Saunders, *Geochem. Geophys. Geosyst.* **8**, Q02006 (2007), doi:10.1029/2006GC001390.
28. C. Herzberg, K. Condie and J. Korenaga, *Earth Planet. Sci. Lett.* **292**, 79 (2010).
29. D. L. Abbott, L. Burgess, J. Longhi and W. H. F. Smith, *J. Geophys. Res.* **99**, 13835 (1994).
30. S. J. G. Galer and K. Mezger, *Precambrian Res.* **92**, 387 (1998).
31. A. H. Knoll, *Geobiology* **1**, 3 (2003).
32. J. K. Willenbring, Al. T. Codilean and B. McElroy, *Geology* **41**, 343 (2013).
33. K. Maher, J. R. Bargar and G. E. Brown, Jr., *Inorg. Chem.* **52**, 3510 (2013).
34. A. Pavlov and J. F. Kasting, *Astrobiology* **2**, 27 (2002).
35. E. C. Pope, D. K. Bird and M. T. Rosing, *Proc. Natl. Acad. Sci.* **12**, 4371 (2012).
36. J. Farquhar, H. M. Bao and M. Thiemens, *Science* **289**, 756 (2000).
37. J. Farquhar, M. Peters, D. T. Johnston, H. Strauss and A. Masterson, *Nature* **449**, 706 (2007).
38. A. J. Kaufman *et al.*, *Science* **317**, 1900 (2007).
39. D. Papineau, S. J. Mojzsis and A. K. Schmitt, *Earth Planet. Sci. Lett.* **255**, 188 (2007).
40. M. T. Rosing and R. Frei, *Earth Planet. Sci. Lett.* **217**, 237 (2004).
41. R. Sharpe and F. Mostafa, *Can. Mineral.* **49**, 1199 (2011).
42. M. Cuney, *Econ. Geol.* **105**, 553 (2010).
43. H. Ohmoto, Y. Watanabe, H. Ikemi, S. R. Poulson and B. E. Taylor, *Nature* **442**, 908 (2006).
44. A. Hofmann, A. Bekker, O. Rouxel, D. Rumble and S. Master, *Earth Planet. Sci. Lett.* **286**, 436 (2009).
45. R. F. Anderson, M. Q. Fleisher and A. P. LeHuray, *Geochim. Cosmochim. Acta* **53**, 2215 (1989).
46. A. Ehrenreich and F. Widdel, *Appl. Environ. Microbiol.* **60**, 4517 (1994).
47. A. Kappler and D. K. Newman, *Geochim. Cosmochim. Acta* **68**, 1217 (2004).
48. N. V. Grassineau, E. G. Nisbet, M. J. Bickle, C. M. R. Fowler, D. Lowry, D. P. Mattey, P. Abell and A. Martin, *Proc. R. Soc. Biol. Sci. Ser. B* **268**, 113 (2001).
49. E. G. Nisbet and C. M. R. Fowler, *Proc. R. Soc. Lond. B* **266**, 2375 (1999), doi:10.1098/rspb.1999.0934.
50. D. E. Canfield and R. Raiswell, *Am. J. Sci.* **299**, 697 (1999), doi:10.2475/ajs.299.7-9.697.

51. J. Xiong, W. M. Fischer, K. Inoue, M. Nakahara and C. E. Bauer, *Science* **289**, 1724 (2000), doi:10.1126/science.289.5485.1724.
52. I. Schröder, E. Johnson and S. de Vries, *FEMS Microbiol. Rev.* **27**, 427 (2003).
53. Y.-S. Luu and J. A. Ramsey, *World J. Microbiol. Biotechnol.* **19**, 215 (2003), doi:10.1023/A:1023225521311.
54. A. M. Mloszewska, S. J. Mojzsis, E. Pecoits, D. Papineau, N. Dauphas and K. O. Konhauser, *Gondwana Res.* **23**, 574 (2013).
55. D. Wacey, M. Saunders, M. D. Brasier and M. R. Kilburn, *Earth Planet. Sci. Lett.* **301**, 393 (2011).
56. T. R. Kulp *et al.*, *Science* **321**, 967 (2008).
57. J. Schott, B. M. Griffin and B. Schink, *Microbiology* **156**, 2428 (2010).
58. A. Cvetkovic *et al.*, *Nature* **466**, 779 (2010).
59. M. Ginder-Vogel, B. Stewart and S. Fendoff, *Environ. Sci. Technol.* **44**, 163 (2010).
60. H. Staudigel, Hydrothermal alteration processes in the oceanic crust, in *Treatise on Geochemistry*, eds. H. D. Holland and K. K. Turekian (Elsevier/Pergamon, 2003), Ch. 3.15 [Vol. 3, edited by R. L. Rudnick, pp. 1511–1535].
61. R. A. Mills and R. M. Dunk, *Geochem. Geophys. Geosyst.* **11**, Q08009 (2010), doi:10.1029/2010GC003157.
62. M. R. Palmer and J. M. Edmond, *Geochim. Cosmochim. Acta* **57**, 4947 (1993).
63. Y. Arai, M. McBeath, J. R. Bargar, J. Joye and J. A. Davis, *Geochim. Cosmochim. Acta* **70**, 2492 (2006).
64. G. C. Dismukes, V. V. Klimov, S. V. Baranov, Yu. N. Kozlov, J. Das Gupta and A. Tyryshkin, *Proc. Natl. Acad. Sci.* **98**, 2170 (2001).
65. J. E. Johnson, S. M. Webb, K. Thomas, S. Onoc, J. L. Kirschvink and W. W. Fischer, *Proc. Natl. Acad. Sci.* **110**, 11238 (2013).
66. M. Ilbert and V. Bonnefoy, *Biochim. Biophys. Acta* **1827**, 161 (2013).
67. Y. Kato, K. Suzuki, K. Nakamura, A. H. Hickman, M. Nedachi, M. Kusakabe, D. C. Bevacqua and H. Ohmoto, *Earth Planet. Sci. Lett.* **278**, 40 (2009).
68. N. H. Sleep, *Int. J. Astrobiol.* **12**, 257 (2012).
69. F. U. Battistuzzi and S. B. Hedges, *Mol. Biol. Evol.* **26**, 335 (2009).
70. F. U. Battistuzzi, A. Feijao and S. B. Hedges, *Evol. Biol.* **4**, 44 (2004), doi:10.1186/1471-2148-4-44.
71. C. E. Blank and P. Sánchez-Baracaldo, *Geobiology* **8**, 1 (2010).
72. N. H. Sleep and D. K. Bird, *Philos. Trans. R. Soc. B* **363**, 2651 (2008).
73. E. Rosa, C. Hillaire-Marcel, B. Ghaleb and T. A. Dick, *Can. J. Earth Sci.* **49**, 758 (2012).
74. J. L. Morford and S. Emerson, *Geochim. Cosmochim. Acta* **63**, 1735 (1999).
75. S. A. Owens, K. O. Buesseler and K. W. W. Sims, *Mar. Chem.* **127**, 31 (2011).
76. J. H. Chen, R. L. Edwards and G. J. Wasserburg, *Geochim. Cosmochim. Acta* **80**, 241 (1986).
77. A. T. Fisher and C. G. Wheat, *Oceanography* **23**, 73 (2010).
78. T. J. Algeo, *Geology* **32**, 1057 (2004).
79. A. J. Dickson, A. S. Cohen and A. L. Coe, *Geology* **40**, 639 (2012).
80. R. Avanzinelli, J. Prytulak, S. Skora, A. Heumann, G. Koetsier and T. Elliott, *Geochim. Cosmochim. Acta* **92**, 308 (2012).
81. K. A. Kelley, T. Plank, L. Farr, J. Ludden and H. Staudigel, *Earth Planet. Sci. Lett.* **234**, 369 (2005).
82. C. Spandler and C. Pirard, *Lithos* **170**, 208 (2013).
83. D. Zhao, Y. Yamamoto and T. Yanada, *Gondwana Res.* **23**, 595 (2013).
84. B. Harte and S. Richardson, *Gondwana Res.* **21**, 236 (2012).

85. A. Stracke and A. W. Hofmann, *Geochem. Geophys. Geosyst.* **6**, Q05007 (2005), doi:10.1029/2004GC000824.
86. Y. Arai, M. McBeath, J. R. Bargar, J. Joye and J. A. Davis, *Geochim. Cosmochim. Acta* **70**, 2492 (2006).
87. J. B. Kellogg, S. B. Jacobsen and R. J. O'Connell, *Earth Planet. Sci. Lett.* **262**, 328 (2007).
88. C. Class and A. Le Roex, *Earth Planet. Sci. Lett.* **305**, 92 (2011).
89. M. Janin, C. Hémond, M. Maia, P. Nonnotte, E. Ponzevera and K. T. M. Johnson, *Geochem. Geophys. Geosyst.* **13**, Q09016 (2012), doi:10.1029/2012GC004165.
90. R. E. Zartman and S. H. Richardson, *Chem. Geol.* **220**, 263 (2005).
91. E. G. Nisbet, D. P. Mattey and D. Lowry, *Nature* **367**, 694 (1994).
92. Z. V. Spetsius, D. F. W. de Vries and G. R. Davies, *Lithos* **112S**, 1032 (2009).
93. M. J. Walter *et al.*, *Science* **334**, 54 (2011).
94. A. Stracke, *Chem. Geol.* **330–331**, 274 (2012).
95. S. L. Goldstein, G. Soffer, C. H. Langmuir, K. A. Lehnert, D. W. Graham and P. J. Michael, *Nature* **453**, 89 (2008).
96. K. E. Donnelly, S. L. Goldstein, C. H. Langmuir and M. Spiegelman, *Earth Planet. Sci. Lett.* **226**, 347 (2004).
97. R. A. Cabral *et al.*, *Nature* **496**, 490 (2013).
98. S. G. Nielsen, M. Rehkamper, M. D. Norman, A. N. Halliday and D. Harrison, *Nature* **439**, 314 (2006).
99. S. G. Nielsen, M. Rehkamper, D. A. H. Teagle, D. A. Butterfield, J. C. Alt and A. N. Halliday, *Earth Planet. Sci. Lett.* **251**, 120 (2006).
100. J. F. Slack and W. F. Cannon, *Geology* **11**, 1011 (2009).
101. J. F. Slack, T. Grenne and A. Bekker, *Geosphere* **5**, 302 (2009).
102. J. F. Slack, T. Grenne, A. Bekker, O. J. Rouxel and P. A. Lindberg, *Earth Planet. Sci. Lett.* **255**, 243 (2007).
103. R. Wirth, F. Kaminsky, S. Matsyuk and A. Schreiber, *Earth Planet. Sci. Lett.* **286**, 292 (2009).
104. F. Kaminsky, R. Wirth, S. Matsyuk, A. Schreiber and R. Thomas, *Mineral. Mag.* **73**, 797 (2009).
105. P. C. Hayman, M. G. Kopylova and F. V. Kaminsky, *Contrib. Mineral. Petrol.* **149**, 430 (2005).
106. M. J. Walter *et al.*, *Science* **334**, 54 (2011).
107. M. Palot, P. Cartigny, J. W. Harris, F. V. Kaminsky and T. Stachel, *Earth Planet. Sci. Lett.* **357–358**, 179 (2012).
108. Y.-I. Liu, B. Zhang, C.-I. Li, F. Hu and B. Vlede, *Soil Sci. Soc. Am. J.* **72**, 1580 (2008).
109. V. Šucha, P. Uhlík, J. Madejová, S. Petit, I. Kraus and L. Puškelová, *Clays Clay Minerals* **55**, 36 (2007).
110. S. R. Boyd, *Precambrian Res.* **108**, 159 (2001).
111. D. Papineau, S. J. Mojzsis, J. A. Karhu and B. Marty, *Chem. Geol.* **216**, 37 (2005).
112. A. Hall, *Earth-Sci. Rev.* **45**, 145 (1999).
113. A. Watenphul, B. Wunder and W. Heinrich, *Am. Mineral.* **94**, 283 (2009).
114. A. Watenphul, B. Wunder, R. Wirth and W. Heinrich, *Chem. Geol.* **270**, 240 (2010).
115. B. Marty and N. Dauphas, *Earth Planet. Sci. Lett.* **206**, 397 (2003).
116. B. Marty and N. Dauphas, *Earth Planet. Sci. Lett.* **225**, 441 (2004).
117. N. Coltice, F. Albarède and P. Gillet, *Science* **288**, 845 (2000).
118. A. A. Borokov, *Probability Theory* (Gordon and Breach, Amsterdam, 1998).

119. E. M. Klein, Geochemistry of the igneous oceanic crust, in *Treatise on Geochemistry*, eds. H. D. Holland and K. K. Turekian (Elsevier/Pergamon, 2003), Ch. 3.13 [Vol. 3, edited by R. L. Rudnick, pp. 433–463].
120. E. M. Klein and C. H. Langmuir, *J. Geophys. Res.* **92**, 8089 (1987).
121. D. McKenzie and M. J. Bickle, *J. Petrol.* **29**, 625 (1988).
122. T. Plank and C. H. Langmuir, *J. Geophys. Res.* **97**, 19749 (1992).
123. C. Herzberg and R. Rudnick, *Lithos* **149**, 4 (2012).
124. J. Blichert-Toft, B. Zanda, D. S. Ebel and F. Albarède, *Earth Planet. Sci. Lett.* **300**, 152 (2010).
125. G. A. Brennecka and M. Wadhwa, *Proc. Natl. Acad. Sci.* **109**, 9299 (2102).
126. J. Hiess, D. J. Condon, N. McLean and S. R. Noble, *Science* **335**, 1610 (2012).
127. S. Weyer, A. D. Anbar, A. Gerdes, G. W. Gordon, T. J. Algeo and E. A. Boyle, *Geochim. Cosmochim. Acta* **72**, 345 (2008).
128. J. M. Herndon, *Proc. Natl. Acad. Sci.* **100**, 3047 (2003).
129. D. C. Bradley, *Earth-Sci. Rev.* **108**, 16 (2011).